KINETICS OF CHARGE TRANSFER AT THE LIPID BILAYER–WATER INTERFACE ON THE NANOSECOND TIME SCALE

MARTIN WOODLE, JING WEN ZHANG, AND DAVID MAUZERALL
The Rockefeller University, New York, New York 10021

ABSTRACT Advances in instrumentation allow electrical measurements across the planar lipid bilayer to be made with nanosecond time resolution. The electron transfer reaction between photoexcited magnesium octaethylporphyrin in the lipid to a variety of ionically charged acceptors in the water is found to be purely dynamic over a wide range of concentrations of acceptors and up to the time constant of the apparatus, 4 ns. The saturation of the amplitude of the photovoltage with increasing concentration of acceptor is caused by the finite lifetime of the excited state, not by formation of a static pigment–acceptor complex. The reactions are an excellent probe of the lipid–water interface over an extended time scale. No appreciable barrier to reaction exists at this interface beyond the 5-ns time. That is, any water or choline group structure may be evanescent on this time scale. Electrostatic interactions indicate that the acceptor molecules penetrate to the level of the phosphocholine groups with differing orientations. It will be possible to extend the time scale into the picosecond range by decreasing the response time and by deconvolutions.

INTRODUCTION

The lipid bilayer–water interface is an excellent example of a self-organized system. The large number of publications on properties of lipid bilayers testifies to the interest and to the richness of the system. Most of this work has concentrated on trans-membrane aspects of the bilayer (Fendler, 1984; Tien and Joshi, 1986; Dannhauser et al., 1986; Flewelling and Hubbell, 1986) and of diffusional motion in the membrane (Davis, 1983). Specific studies of the interface itself are less common (Hong, 1976; Liu and Mauzerall, 1985; Watts and Poile, 1986), yet the interfacial region is very likely more complex and structured than the hydrocarbon core (Davis, 1983; Smith and Oldfield, 1984). Many biological reactions of interest, such as ion and substrate transport, integral protein insertion, and cell adhesion factors, must pierce this interface. Thus its properties may be crucial to many biological processes.

Photoinduced electron transfer across the lipid bilayer–water interface is a sensitive and specific method to study that interface with high time resolution (Hong and Mauzerall, 1976; Varnadore et al., 1982). It is precisely the interface that allows vectorial electron transfer in planar bilayers and thus its measure by sensitive electrical methods. The steep gradient of polarity at the interface allows simple separation of ionic acceptors and hydrophobic donors or vice versa. If the donor is a hydrophobic, photoreactive pigment and the acceptor is present on only one side of the bilayer, one can show that the measured charge transfer is specific to a single interface in the bilayer portion of a Rudin–Mueller membrane (Hong and Mauzerall, 1972). Essentially one is working with a test tube 5–10-Å deep having a definite structure and orientation.

Our studies have given information on the localization of pigment molecules at the interface and on the low mobility of the porphyrin cation (Woodle and Mauzerall, 1986). Electrostatic properties and autopolarization effects at the interface have been calculated (Raudino and Mauzerall, 1986). The decay of the photoinduced voltage shows distributed function kinetics explained as a distribution of distances between the oxidized donor and the reduced acceptor (Liu and Mauzerall, 1985).

Here we have used a fast electrical system to time resolve the forward electron transfer, i.e., from excited lipidic porphyrin to the aqueous acceptor. The forward electron transfer rates have been measured with various concentrations of several different electron acceptors, both anionic and cationic, with and without oxygen present, and at different concentrations of the pigment in the bilayer. The apparent second-order rate constants are near the encounter limit for homogeneous reaction in water, indicating no appreciable barrier to reaction at the interface. Their variation with the charge of the acceptor and the ionic strength of the solution can be explained by differing orientation of the acceptors at the interface.

MATERIALS AND METHODS

Lipid Bilayers

The Mg octaethylporphyrin (MgOEP) containing bilayers were prepared as described before (Ilani and Mauzerall,

1981; Woodle and Mauzerall, 1986). Briefly, MgOEP was dissolved to a concentration of 4 mM in a decane solution containing 3% wt/vol L-α-lecithin (Avanti Polar Lipids, Inc., Birmingham, AL) with 0.8% wt/vol cholesterol (Sigma Chemical Co., St. Louis, MO). The bilayer was formed by the brush method across a 1.6-mm hole in a Teflon partition (Mueller et al., 1963). The aqueous solution was buffered with 10 mM KPO_4, pH 6.8, containing 1.0 M NaCl, except as indicated. Concentrated solutions of electron acceptors were added to one aqueous phase: ferricyanide (FeCy), methyl viologen (MV) (Aldrich Chemical Co., Milwaukee, WI; and Sigma Chemical Co.), and recrystallized sodium anthraquinone-2-sulfonate (AQS) or anthraquinone-2,6-disulfonate (AQDS). The oxygen concentration was lowered to $<10^{-7}$ M. This was determined by measurement of triplet lifetimes by delayed luminescence (Ilani et al., 1985) after addition of glucose oxidase (0.13 mg/ml; U.S. Biochemical, Cleveland, OH), catalase (0.066 mg/ml; Sigma Chemical Co.), and glucose (13 mM) to both aqueous phases.

Electrical Measurements

Charge transfer across an interface of a bilayer results in a measurable voltage or current induced in electrodes placed in the separated aqueous phases. For charge transfer across a single interface, the observable voltage will be attenuated because of the capacitative coupling to the second interface. The interfacial or chemical (Hong and Mauzerall, 1974) and membrane capacitances combine to form a capacitative divider. The charge on this chemical capacitance and thus on the whole membrane is a quantitative measure of the charge transfer reaction. The measured voltage is directly proportional to this charge as long as the charge inside the bilayer does not move. Since the change of observed voltage is small for distances of ~5 Å near the interface, it can be neglected for the present. The high resistance of the bilayer membrane ($R_m \sim 10^8$ Ω) requires that an amplifier with even higher input resistance be used for measurements close to the membrane time constant, $R_mC_m \sim 1$ s. However, the membrane impedance decreases with increasing frequency because of its large parallel capacitance, $C_m \sim 5$ nf, e.g., between 1 and 100 MHz the membrane impedance decreases from 2,000 Ω to 20 Ω. Thus although the impedance of most amplifiers also decreases at high frequencies, it need only be larger than that of the membrane in the desired frequency range. However, the access impedance, R_a, i.e., the impedance of all material between the membrane and amplifier input, such as electrodes and solution, is in series with the membrane. This impedance must also be kept below the amplifier impedance. High salt concentration and small electrode-bilayer distance serve this purpose. If one is willing to forego DC measurement, polarizable, i.e., capacitative, electrodes are a simple solution. Small platinum (Pt) wires are nonphotoactive and their capacitance can be kept relatively small. To include DC measurements, low resistance (~100 Ω) calomel electrodes can be used. If these requirements are met, the system response will be linear over the needed frequency range. A differential amplifier is most useful to reject common mode noise, e.g., laser artifact. Even so, adequate shielding is mandatory.

The present apparatus uses a commercial amplifier: a differential probe (model P6046; Teletronix, Inc., Beaverton, OR) of 100-MHz bandwidth and nominal 1-MΩ impedance, decreasing to 2 KΩ at 100 MHz. The Pt electrodes (1-cm long by 0.025-cm diam) are directly connected to the inputs and the probe is positioned directly above the membrane support with the Pt wires close to the membrane but out of the light path. Electrodes containing silver, such as BNC connectors, produce large photo artifacts and their shielding is difficult. Because of the large electromotive force developed by asymmetrical solutions of electroactive acceptors, e.g., FeCy, the amplifier is usually AC coupled. The output of the amplifier was digitized by a Biomation 8100 transient recorder (10-ns minimum sample time), averaged in a Data 6000 computer, stored on disks, and analyzed by a Hewlett-Packard 86 computer (Hewlett-Packard Co., Palo Alto, CA). The system rsponse was 60 ns, limited by the digitizer amplifier. For fastest response, the amplifier output was digitized and averaged by a Tektronix 7912AD scan converter (10-ps minimum sample time) and stored and analyzed on a Hewlett-Packard 9825A computer. This system response is limited by that of the probe, 4 ns. The response to an applied square wave is shown in Fig. 1. The recordings were triggered by the light pulse itself through a fast photodiode. The light pulse was a 7-ns pulse from a nitrogen laser (Molectron UV1000) pumping a homemade dye laser. The dye was usually Rhodamine 6G, with output at 560 nm, 0.3 mJ.

The difficulty with the measurement is that the observed photovoltage is ~1 mV, so a gain of 10 or more is needed to obtain sufficient bits (~6) in the digitization for efficient averaging. Thus not only an impedance converter is necessary, but it must have gain at 100 MHz. The averaging is needed because it is difficult to reduce noise at 100 MHz bandwidth to <0.25 mV.

RESULTS

The rise of the photovoltage across the bilayer after a pulse of light measured by the Tektronix 7912 AD is shown in Fig. 1. The polarity of the photovoltage is such that the aqueous phase containing the electron acceptor becomes negative with respect to the other aqueous phase, in agreement with the view that the excited pigment transfers an electron to the aqueous acceptor forming the cation P^+ in the lipid bilayer. The signal amplitude increases hyperbolically with FeCy concentration in agreement with earlier studies (Ilani and Mauzerall, 1981). The hyperbolic relationship can be described by two parameters: V_{max}, the maximum photovoltage, and K, the concentration of acceptor at which half of the maximum photovoltage is

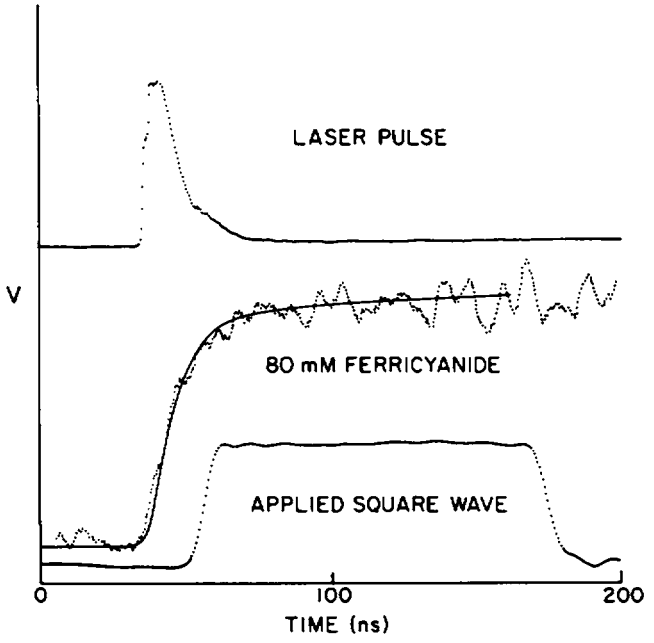

FIGURE 1 (*Top*) Photodiode response to the nitrogen pumped 560-nm dye laser excitation pulse. (*Middle*) Photovoltage rise produced by MgOEP containing bilayer in the presence of 80 mM FeCy on one side under standard conditions. The data are an average of 128 sweeps. The amplitude is 1 mV, negative in the FeCy-containing side. The MgOEP concentration is 4 mM in the membrane-forming solution. The solid line is a convolution of the light pulse with a 4-ns amplifier risetime. (*Bottom*) MgOEP containing bilayer and amplifier response to a low impedance square wave voltage source. Data acquired with Tektronix 7912AD/HP9825. The points are spaced at 0.4 ns.

observed. Plots of the inverse amplitude versus inverse concentration were used to obtain K and are listed in Table I. The saturation constants are similar to earlier measurements (Ilani and Mauzerall, 1981; Ilani et al., 1985). The time for the photovoltage to decay to one-half the maximum with FeCy, MV, and AQS is in agreement with earlier values (Liu and Mauzerall, 1985). As observed before, V_{max} is roughly independent of the acceptor. No photovoltages are observed on illumination if the bilayer is broken, if the porphyrin is not added to the membrane-forming solution, or before the aqueous electron acceptor is added. Thus various artifacts are negligible. The amplitude of the photovoltage is linearly dependent on the light intensity at low intensities but saturates at higher intensities. Since we are not able to fully saturate the photoeffect, theoretical fits to the light saturation data remain ambiguous. The instrumental system response is thus linear and the photovoltage is a good measure of the interfacial electron transfer from the MgOEP in the bilayer to the aqueous electron acceptor. The results obtained with each of the three electron acceptors will be described separately.

Ferricyanide (FeCy)

The photovoltage increases to −4 mV at saturating concentrations of FeCy and partially saturating light. The rate constant of the photovoltage rise is obtained from plots of the complement of the normalized photovoltage on a log scale versus time (Fig. 2). With the best S/N plots can be linear over almost two decades, 98% of the rise. Thus the photovoltage rise is fit with a single, pseudo first-order rate constant. The pseudo first-order rate constant increases linearly from 1 to 100 μs^{-1} as the FeCy concentration is increased from 0.05 to 20 mM (Fig. 3). The slope of the linear fit to the data in Fig. 3 is an apparent second-order rate constant of $1.5 \pm 0.1 \times 10^9\ M^{-1}s^{-1}$ with a finite rate of 0.4 μs^{-1} at infinite dilution of the acceptor.

When oxygen is removed from the aqueous phase, the risetime can again be fit with a single exponential rate constant (Fig. 2). The rate constant is again linear with FeCy concentration, and only slightly changed: $0.9 \pm 0.1 \times 10^9\ M^{-1}s^{-1}$ (Fig. 3). However, the intercept at

TABLE I
RATE AND SATURATION CONSTANTS FOR ELECTRON TRANSFER FROM MgOEP TO VARIOUS ACCEPTORS IN LECITHIN BILAYERS

Acceptor	K_1k_2	$k_1 + k_oO_2$	K	$\frac{k_1 + k_oO_2}{K_1k_2} = K$
	$10^9\ M^{-1}s^{-1}$	$10^6\ s^{-1}$	mM	mM
FeCy, air	1.5	1.0	0.5	0.7
FeCy, $-O_2$	0.9	~0.05	~0.2	0.05
FeCy, low MgOEP, air	1.1	1.1	0.6	1.0
FeCy, low MgOEP, $-O_2$	1.2	~0.1	0.3	0.1
MV, air	0.053	1.1	30	20
MV, $-O_2$	0.048	<0.05	2	<1
MV, $+O_2$	0.05	2.5	~80	50
MV, low MgOEP, $-O_2$	0.04	0.07	1	2
AQS, air	50	1.5	0.03	0.03
AQDS, air	0.3	0.8	—	2.7

The standard conditions were 1 M NaCl and 10 mM phosphate buffer, pH 6.8, with 2 mM MgOEP in the membrane-forming solution. Oxygen was removed or added as described in the experimental section. The experiments with low MgOEP had one-tenth the usual concentration. Solubility limited the ability to saturate the reaction with AQDS.

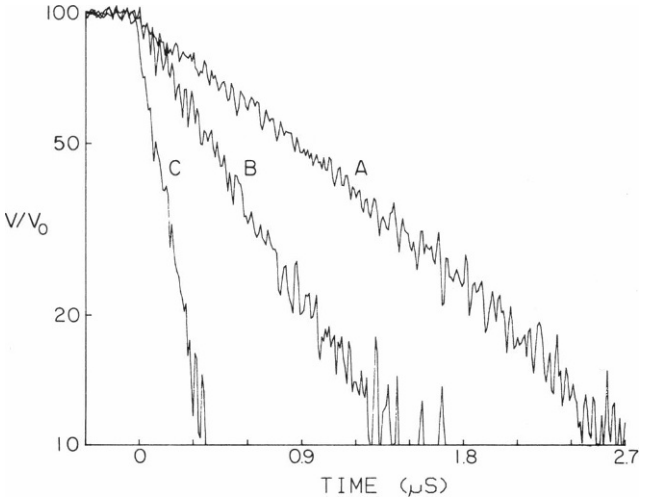

FIGURE 2 Plot on a log scale of the complement of the photovoltage rise normalized to 100. Data acquired with Biomation 8100/Data 6000, 128 sweeps averaged. (*A*) 0.5 mM FeCy in the absence of O_2; (*B* and *C*) 0.5 mM and 5 mM FeCy, respectively, in air-saturated buffer, pH 6.8, 1 M NaCl, 25°C. The pseudo first-order rate constant (k_1) is obtained from the slope of these data.

infinite dilution of the acceptor is near zero. Removing oxygen increases the photovoltage amplitude at low FeCy concentrations but not at high concentrations (Ilani et al., 1981). This is expected from the decrease in K (Table I).

Methyl Viologen (MV)

Similar results are obtained with MV as the electron acceptor. A graph of the photovoltage rise is shown in Fig. 4. The log plot shows that the data can also be fit with a single exponential. The first-order rate constant is linearly dependent on the MV concentration (Fig. 5). The linear fit

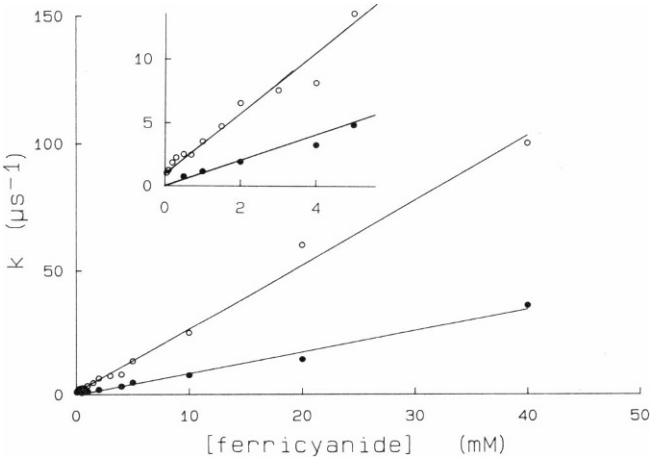

FIGURE 3 Plot of the pseudo first-order rate constant (k_1), obtained from plots as in Fig. 2, as a function of acceptor concentration (FeCy). The slope of the linear fit to the data is the second-order rate constant, $K_i k_2$. The inset is a magnified portion of the figure. O, air; ●, absence of O_2.

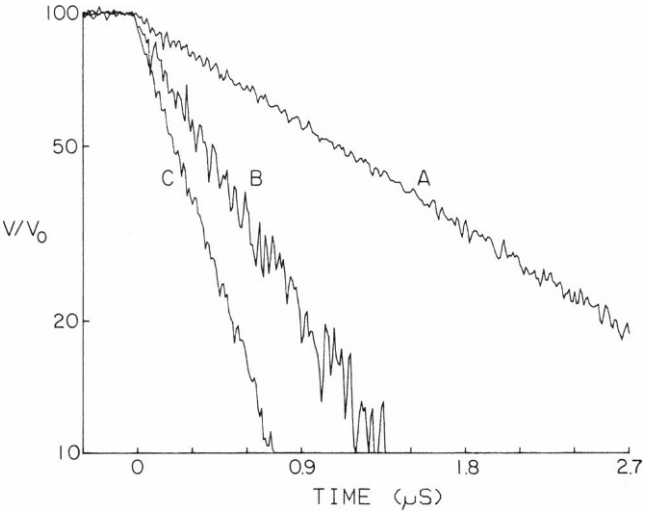

FIGURE 4 Plot of data as in Fig. 2 obtained with MV as the acceptor. (*A*) 10 mM MV in the absence of O_2; (*B*) 10 mM MV in the presence of air; (*C*) 80 mM MV in the absence of O_2.

to the data in Fig. 5 gives an apparent second-order rate constant of $4.2 \pm 0.5 \times 10^7\ M^{-1}s^{-1}$ with a finite rate of 1 μs^{-1} at infinite dilution of the MV. The amplitude of the photovoltage is hyperbolically dependent on the MV concentration, and the data can be fit with a K of 30 mM (Table I). The maximum photovoltage observed with saturating MV and near saturating light was typically −4 mV, similar to that with FeCy.

When oxygen is removed, the photovoltage rise can be fit with a single exponential rate constant that is linearly dependent on the MV concentration as shown in Fig. 5. The fit to the data in Fig. 5 gives a second-order rate constant identical to that when oxygen is present but with an intercept of near zero at infinite dilution of the MV. Measurements at higher oxygen concentrations than air were incomplete because it is difficult to maintain the

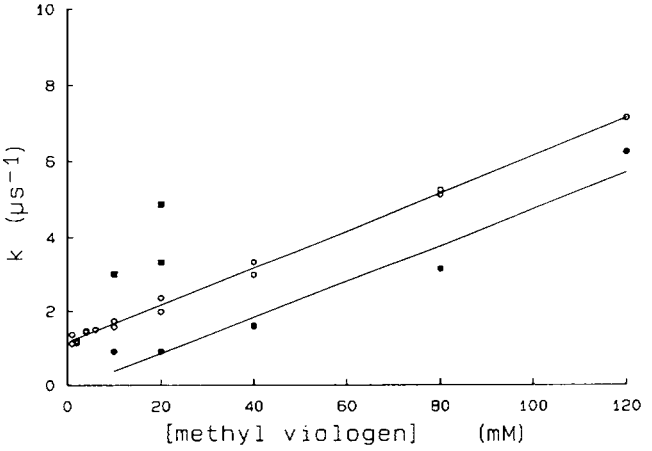

FIGURE 5 Plot of pseudo first-order rate constants as a function of MV concentration as in Fig. 3. O, air-saturated 1.0 M NaCl; ●, same, in the absence of O_2; ■, same, increased O_2.

increased oxygen concentration. Nevertheless, the results are consistent with the same second-order rate constant and an increase in the rate constant at infinite dilution of MV (see Fig. 5). In addition, the amplitude increases by a factor of ~2 upon removing oxygen at low MV concentrations, similar to FeCy.

Anthraquinone-2-Sulfonate (AQS)

The use of AQS as the electron acceptor also results in a photovoltage that has the characteristics expected from the earlier measurements (Fig. 6 and Table I). The amplitude is only slightly smaller than that produced by FeCy or MV but the half saturating concentration is much lower, 0.1 mM. The rise of the photovoltage is again fit by a single exponential (Fig. 6) and this rate constant is a linear function of concentration of AQS (Fig. 7). The apparent second-order rate constant is very high, 10^{11} $M^{-1}s^{-1}$. The finite intercept at zero AQS concentration is 1 μs^{-1}.

Anthraquinone-2,6-Disulfonate (AQDS)

Since we had conjectured that the large difference in the saturation constants for the reaction with AQS and AQDS was the amphoteric nature of the former (Ilani et al., 1985), it was of interest to observe the difference in reactivity as measured by the second-order rate constant. The data in Table I show that this constant for AQDS is fully 100 times smaller than that of AQS. The half saturation constant also increases by at least 20-fold. Solubility of the AQDS limited the measurements. Again the risetimes are monoexponential and the removal of oxygen had a small effect.

Negatively Charged Lipid

Dimyristoyl glycerol phosphoserine (DMPS) was added to the egg lecithin to determine the effect of fixed charges at the lipid–water interface. The data with and without 10% DMPS and at two ionic strengths are listed in Table II. Decreasing the ionic strength 30-fold did not change either the second-order rate constant or the saturation constant for the negative acceptors with lecithin bilayers. These constants did increase threefold and decrease fivefold, respectively, with the positive acceptor MV.

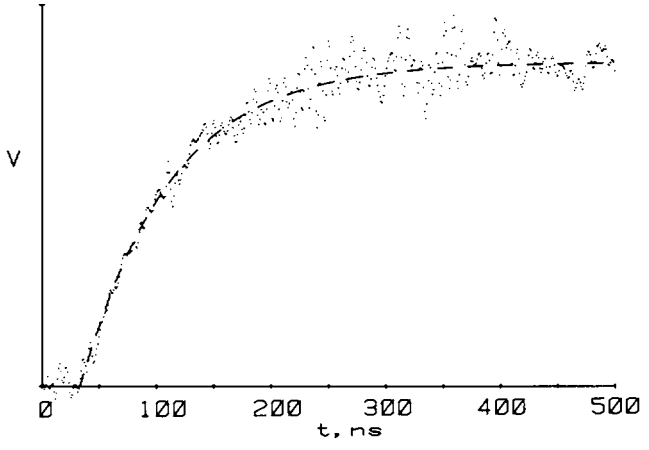

FIGURE 6 Plot of rise of photovoltage from 0.2 mM AQS. The dashed line is an exponential fit, τ = 78 ns.

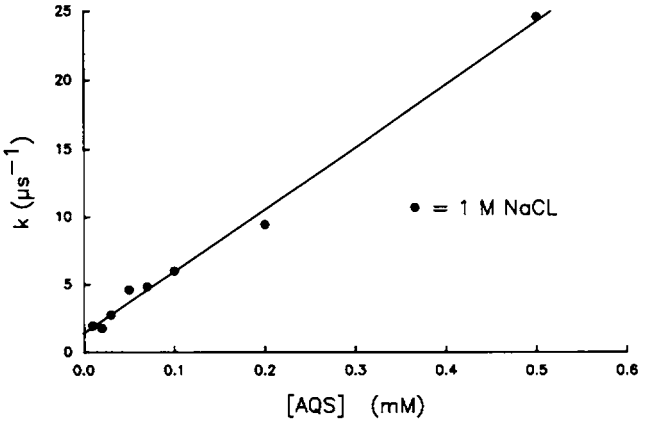

FIGURE 7 Plot of pseudo first-order rate constant as a function of AQS concentration in air as in Fig. 3.

DISCUSSION

We identify the photovoltage with the amount of charge on the chemical or interfacial region capacitance (Hong and Mauzerall, 1976), itself capacitatively coupled to the membrane capacitance. The charge on the latter is that of the porphyrin cation in the interfacial region. The increased time resolution of the present experiments allows measurement of the forward electron transfer rate, i.e., the rate of charge transfer from the excited pigment in the bilayer to the aqueous acceptor across the interface. The charge transfer reaction may be dynamic or static, i.e., the excited pigment or intermediate may react with the acceptor at a rate proportional to their respective concentrations, or the two reactants may form a complex in the dark, and react on photoexcitation. In the steady state, both of these mechanisms lead to a hyperbolic saturation of photovoltage (V) with acceptor (A). Previous measurements of the amplitude of the photovoltage showed such a behavior, and the dynamic case was inferred by other arguments (Ilani and Mauzerall, 1981). The present data (Figs. 3, 5, and 7) clearly show that the reaction is dynamic: the pseudo first-order rate constant for the voltage rise is a linear function of the acceptor concentration well past (20–100-fold) that required for saturation. The risetime would be independent of the acceptor concentration in the amplitude saturated range if the photoexcited static P...A complex were required to transfer charge. This is quite analogous to Stern–Volmer kinetics of the quenching of fluorescence. The same conclusion holds for the dynamic case if the escape of the $P^+...A^-$ pair to form a voltage were rate determining. Thus the reaction is not static.

TABLE II
IONIC EFFECTS ON RATE CONSTANTS FOR ELECTRON TRANSFER FROM MgOEP TO VARIOUS ACCEPTORS IN LECITHIN BILAYERS

μ, M	0% DMPS				10% DMPS			
	1.0		0.035		1.0		0.035	
	k_2K_i	K	k_2K_i	K	k_2K_i	K	k_2K_i	K
Acceptor	$10^9\ M^{-1}s^{-1}$	mM	$10^9\ M^{-1}s^{-1}$	mM	$10^9\ M^{-1}s^{-1}$	mM	$10^9\ M^{-1}s^{-1}$	mM
FeCy (−3)	1.1	0.6	0.9	0.8	0.9	2	0.2	8
AQS (−1)	50	0.03	40	0.03	36	—	3.5	0.1
MV (+2)	0.05	20	0.16	4	0.045	6	0.3	0.5

Conditions as Table I except ionic strength, μ, varied: 1 M NaCl + 10 mM $NaPO_4$, pH 6.8, or 0.01 M NaCl + 10 mM $NaPO_4$, pH 6.8. The percent DMPS is the percentage of dimyristoyl-glycero-phosphorserine in the lipid-forming solution, the remainder being lecithin.

In contrast to the single exponential photovoltage formation, the kinetics of the photovoltage decay are complex, requiring a distributed function to be explained (Liu and Mauzerall, 1985). Our explanation of the difference of the forward and reverse kinetics at the bilayer interface is based on the demonstration that the critical radius for encounter limited reactions in the excited state is considerably larger (7 Å for porphyrins) than that for ground state molecules (Ballard and Mauzerall, 1980; Mauzerall and Ballard, 1982). Thus the reverse reaction requires movement in the interfacial region of donor inwards, and/or of the porphyrin cation outwards, on the longer time scale. Calculations indicate that it is the donor that moves (unpublished). The resulting distribution of distances (if simple tunneling is the mechanism) or of activation energies leads to characteristic distributed kinetics for the photovoltage decay.

Mechanism

The dynamic mechanism is

$$P \xrightarrow{\phi\sigma E} P^* \quad (1)$$

$$P^* \xrightarrow{k_1} P \quad (2)$$

$$P^* + O_2 \xrightarrow{k_0} P + O_2 \quad (3)$$

$$P^* + \cdots A \xrightarrow{k_2} P^* \cdots A^- \quad (4)$$

$$P^+ \cdots A^- \xrightarrow{k_3} P^+ + A^- \quad (5)$$

$$\cdots + A \underset{k_i}{\rightleftharpoons} \cdots A \quad (6)$$

The $\cdots$ symbol refers to the interfacial region and so Eq. 6 is a distribution function of the acceptor between this region and the aqueous solution. It is assumed that the porphyrin relevant to the experiment is already in this region since it moves relatively slowly in the membrane (Woodle and Mauzerall, 1986). The formation of the photovoltage after a nonsaturating flash of duration less than the relevant time constants, assuming k_3 is fast, is given by

$$C\Delta V/vF = P^+ = \phi\sigma E PA(1 - e^{-kt})/(K + A) \quad (7)$$

$$k = k_1 + k_oO_2 + K_ik_2A \quad (8)$$

$$K = (k_1 + k_oO_2)/K_ik_2, \quad (9)$$

where ϕ is the quantum yield of the reactive state, σ is the optical cross-section for the pigment, and E is the fluence of the flash. K_i contains the intermolecular interaction energies (and entropies) which favor or disfavor the accumulation of A at the interface. The left-hand term converts electral units to concentration of P^+: C is the capacitance, ΔV the observed voltage, v the volume of the interfacial region, and F the Faraday constant.

This mechanism predicts the observed hyperbolic saturation of the photovoltage with increasing acceptor, A, with a saturation constant, K. Eq. 9 predicts a linear correlation of K with $1/K_ik_2$. This is found to be so within a factor of two over three orders of magnitude in K for differing acceptors (Table I, third and first columns). There is good agreement between the observed K obtained from measurements of photovoltage amplitude and that calculated from the rise kinetics (Table I, third and fourth columns). The mechanism predicts that the exponential rise of the photovoltage (Eq. 7, Figs. 2, 4, and 6) will be a linear function of A beyond the value $1/K$ (Eq. 8, Figs. 3, 5, and 7). The finite intercept of this plot is a function of O_2 concentration (Eq. 8, Figs. 3 and 5). This intercept is the lifetime of the photoformed intermediate P*, ~1 μs in air but much longer in the absence of oxygen.

The most likely intermediate is the triplet state of the porphyrin, which is quenched by O_2 with a typical rate constant of $3 \times 10^9\ M^{-1}s^{-1}$, and has a lifetime, $1/k$, of 10^{-3} s. The fit of our limited O_2 data yields a k_o of $10^9\ M^{-1}s^{-1}$ and a k_1 of $<10^5\ s^{-1}$. This is insufficient to rule out a different mechanism wherein loose clusters of porphyrins

in the triplet and ground-state ionize, forming P^+ and P^- (Ilani and Mauzerall, 1981). The latter could be the intermediate which would react with O_2 or with A. Some evidence against this auto-ionization mechanism is seen in the data where the membrane-forming solution contains only one-tenth as much porphyrin (Table I). The $K_i k_2$ and K for various A's are the same, indicating no change in reacting species. The yield of photovoltage decreases by only about one-half on dilution. The most likely explanation is that a large degree of concentration quenching occurs at the higher concentration, and this reaction produces few ions. However, it cannot be completely excluded that the porphyrin has limited "solubility" in the bilayer and thus the actual bilayer concentration is not proportional to solution concentraton (Cherry et al., 1972). Since the fluorescence of MgOEP in lecithin liposomes is 50% quenched at 1 mM AQS (Ilani et al., 1985), the constancy of the second-order rate constant $K_i k_2$ (Fig. 7) and of the photovoltage (data not shown) into this region strongly suggests that the singlet state can also react with equal efficiency to form stabilized ions, i.e., a photovoltage. Since the reverse reaction to the ground state is spin allowed in this transition, the observed yield must be caused by the enforced separation of the product ions (Mauzerall and Ballard, 1982).

Electrostatics

The choice of anionic, cationic, and amphoteric acceptors was made to differentiate electrostatic effects at the lecithin–water interace. In earlier work using voltage amplitudes (Ilani and Mauzerall, 1981), the cause of the large K of the cationic MV compared with FeCy was assigned to repulsion by the cationic choline group, and the enhanced reactivity of AQS to its amphoteric nature: the hydrophobic end penetrates into the interfacial region. The present kinetic experiments modify the former and reinforce the latter conclusions.

In free solution, these acceptors react rapidly with triplet states of porphyrins. Typical data are shown in Table III. Zinc uroporphyrin (-8 charge) reacts with FeCy ion in water with a rate constant of 2×10^8 $M^{-1}s^{-1}$ when corrected for electrostatic effects (Carapellucci and Mauzerall, 1975). We showed at that time that "repulsive" collisions, which slowed the forward rate of reaction, could increase the yield of escaped ions (quantitative in the above case) by increasing the escape rate. Quinones in general react at encounter limited rates, e.g., triplet Zn and Mg tetraphenyl porphyrins and benzoquinone in ethanol, have rate constants of 3×10^9 $M^{-1}s^{-1}$ (Harriman et al., 1983*b*). Interestingly, triplet zinc protoporphyrin (-2 charge) and benzoquinone (0 charge) in ethanol-water have a reaction rate constant of 7×10^9 $M^{-1}s^{-1}$, but that with naphthoquinone sulfonate (-1 charge) is an order of magnitude less (Feitelson and Barboy, 1986). Reaction of zinc tetra-*N*-methyl-pyridinium porphyrin ($+4$ charge) with MV ($+2$ charge) in water has a rate constant of 2×10^7 $M^{-1}s^{-1}$, while the reaction with triplet zinc tetra-phenyl-sulfonate porphyrin (-4 charge) is quoted as 10^{10} $M^{-1}s^{-1}$ (Harriman et al., 1983*a*). The latter is a case of reaction from a preformed "static" complex, with a dissociation constant of $>10^9$ M^{-1} (Nahor and Rabani, 1985). Thus electrostatic effects in free solution are appreciable. Electrostatic effects on the quenching of chlorophyll triplets in lecithin vesicles have been investigated by flash photolysis (Senthilanthipan and Tollin, 1985). Data at only a single acceptor concentration were collected. This and the complex kinetics make it difficult to draw clear conclusions. However, the halflives of the triplet chlorophyll were relatively unchanged on adding dihexadecyl phosphate (0–30%) in the presence of 0.2 M phosphate using either MV or AQS as acceptor. Substitution of 0.05 M betaine

TABLE III
ELECTROSTATIC EFFECTS IN ELECTRON TRANSFER REACTIONS OF PHOTOEXCITED PORPHYRINS

Porphyrin	Charge	Acceptor	Charge	Solvent	k_2	$K_i k_2$, 1 M NaCl
					10^9 $M^{-1}s^{-1}$	10^9 $M^{-1}s^{-1}$
ZnURO*	−8	FeCy	−3	H_2O, $\mu = \infty$	0.2	1
ZnURO	−8	FeCy	−3	H_2O, $\mu = 0$	0.00054	
ZnP (NMepyr)‡	+4	MV	+2	H_2O	0.02	
ZnP (ϕSO_3)‡	−4	MV	+2	H_2O	>10	0.05
Zn or MgPϕ‡	0	Benzoquinone	0	Ethanol	3	50 (AQS)
Zn Proto‖	−2	Benzoquinone	0	Ethanol H_2O	7	
Zn Proto	−2	Naphthoquinone-sulfonate	−1	Ethanol H_2O	0.7	0.3 (AQDS)

URO is uroporphyrin III; P (NMepyr)$_4$ is tetra-meso [4-(*N*-methyl pyridinium)] porphyrin; P(ϕSO_3)$_4$ is tetra-meso-[4-sulfonato phenyl] porphyrin; Pϕ_4 is tetra-meso-phenyl-porphyrin; and Proto is protoporphyrin IX.

*Carapellucci and Mauzerall, 1975.

‡Harriman et al., 1983a.

§Harriman et al., 1983*b*.

‖Feitelson and Barboy, 1986.

for the phosphate buffer did cause a shortened lifetime of the chlorophyll triplet by MV with increasing percentage of the negatively charged lipid. These observations are similar to those shown in Table II.

Before comparison of the rate constants of the interfacial reactions we must consider the value of K_i, the distribution coefficient of the acceptor between bulk aqueous and interfacial membrane regions. It is known that large hydrophobic ions are bound at the bilayer–water interface of phospholipids, with the anions being highly favored (the binding constant of ϕ_4P^+ is $\sim 10^2$, of ϕ_4B^- $\sim 10^6$, Flewelling and Hubbell, 1986). The amphiphilic AQS is known to bind to micelles of lauryl sulfate (Kano and Mastuo, 1974) and our observation of K_ik_2 greater than the encounter limit for AQS implies binding. The binding constant of the similar 2-toluido-naphthalene-6-sulfonate (TNS) to lecithin vesicles is 3×10^{-5} M with a maximum binding of 1/550 Å^2 (Huang and Charlton, 1972), although McLaughlin (1977) obtained a better fit to the data using the Gouy–Chapman model with a K of 2×10^{-4} M and a surface charge density of 1/70 Å^2.

In contrast, it is unlikely that the smaller and more highly charged FeCy ion can bind as strongly to a lecithin bilayer. The binding property of the dianion AQDS would presumably be intermediate but closer to FeCy because of the lack of definite amphiphilicity. The binding constant of the dication MV has been approximated by kinetic analysis of chlorophyll-containing liposomes. As expected, its value ranges from 0.2 (Ford and Tollin, 1986*a*) to 1 (Ford and Tollin, 1986*b*). Thus there is no evidence for binding in these cases. We are now attempting such measurements with AQS.

It must be noted that although one speaks of "binding" to the bilayer, one really means an increased concentration in that region, since the fact that the reaction is dynamic shows that the acceptor is still free to move in this region. Whether the movement is in 2 (surface) or 3 (region) dimensions remains to be seen. Comparison of the data in Tables I and III shows that the rate constant for reaction in 1 M NaCl of triplet MgOEP with tri-anionic ferricyanide has been enhanced by a factor of 5, that with monoanionic AQS by a factor of 20, that of dianionic AQDS inhibited by a factor of 10, and that of dicationic MV has been inhibited by a factor of >50 over corresponding reactions in solution. In fact MV reacts at about the same rate as with the quadruply cationic zinc tetra-*N*-methyl-pyridinium-porphyrin (Table III). The rate constant for the quenching of chlorophyll triplets in lecithin liposomes by MV is 2×10^7 M^{-1}s^{-1} (Ford and Tollin, 1986*a*), about one-half that shown in Table I.

Lowering the ionic strength 30-fold has little effect on the reaction of FeCy or AQS (Table II) but increases the rate constant of MV by a factor of 3. In 1 M salt the addition of 10% DMPS has essentially no effect (Table II). However, on lowering the ionic strength, the rate constants for FeCy and AQS are decreased 5-fold and 10-fold, respectively, while that of MV is increased 7-fold. The saturation constants roughly follow the inverse sequence. Addition of negatively charged lipid has the expected ionic effects at lower ionic strength.

We had earlier explained the low saturation constant for reaction with MV dication as a repulsion with the local phosphocholine dipole. The limited data at lower ionic strength suggest an attractive potential. However, more complete data show a maximum in rate constant near μ = 0.1 (in preparation). Thus a more complex interaction is present. This does not explain the magnitude of the rate constants. A possible explanation is that the MV approaches with its plane parallel to the membrane. The average spacing of the negative phosphate groups, ~14 Å, roughly matches the two positive nitrogens (~10 Å) in MV. Since the porphyrin is held roughly perpendicular to the membrane surface, the required π-orbital overlap would be minimal since the orbitals of the porphyrin and MV are nearly orthogonal (Mauzerall, 1976). A similar orientation of AQDS dianion, now matching the positive choline groups, would also explain its low rate constant. The effect may be weaker in this case because of the movement of the choline ends of the dipole, resulting in a more diffuse potential than that from the more localized phosphate groups. The high symmetry of FeCy eliminates any orientational requirements.

The anomalously high rate constant with AQS may support the orientation hypothesis. This second-order rate constant (Table I), greater even than that calculated for an encounter limited reaction in a low viscosity solvent (10^{10} M^{-1}s^{-1}), can be explained by an increased concentration, i.e., binding, of AQS at the interface. This was previously inferred from the very low value of the saturation constant (Ilani and Mauzerall, 1981). The striking difference from AQDS is due to the amphoteric nature of AQS. In turn, this implies that the hydrophobic end penetrates the interface and this interaction accounts for most of the increased interfacial concentration. The long axis of AQS is held roughly perpendicular to the membrane and thus parallel to the porphyrin plane. The orbital overlap is favored and both this overlap and the reduced intermolecular distance would cause rapid electron transfer. The remarkable 2,000-fold increase in quenching constant for chlorophyll triplets in lecithin liposomes by di-octyl viologen over MV (Ford and Tollin, 1986*a*) can be explained by its insertion in this similar perpendicular orientation.

The zeroth approximation to these electrostatic effects is that they represent the effect on the binding constant, K_i, of the interaction between a surface charge on the membrane and the charge on the acceptor:

$$K_{i\mu}/K_{i1} = \exp\left[-Z_ie(\psi_\mu - \psi_1)/kT\right], \qquad (10)$$

where $K_{i\mu,1}$ and $\psi_{\mu,1}$ are the binding constant for the ith acceptor and the surface potential at ionic strength μ and 1, respectively, and Z_i is the charge on the ith acceptor. An

estimate of the surface potential for the bilayer containing 10% PS is -50 mV at $\mu = 0.035$ and -9 mV at $\mu = 1$ (for Gouy–Chapman–Stern equations and units see McLaughlin, 1977). With AQS, ($Z = -1$) the ratios of observed K_1k_2 is 0.1, and that of calculated K_1k_2 is 0.2. Thus the AQS is inserted in the membrane and the sulfonate group is close to the hypothetical Gouy–Chapman surface. However, the same ratios are seriously in error for FeCy (obs. 0.2, calc. 0.002) and MV (obs. 7, calc. 50). Adequate fit can be obtained by placing these ions at ~10 Å (FeCy) and 5 Å (MV) from the Gouy–Chapman surface. A more adequate model must incorporate the finite size of the ions and treat the problem self consistently as diffusion in the face of a potential, following Debye (1942; see Mauzerall and Ballard, 1982). We are now doing this with a more complete data set on these reactions.

The distinction between smeared charge (Gouy–Chapman) models and discrete charge models of a polarized nonmetallic interface can probably be most clearly made by reference to the ratio of intercharge distance on the membrane to the Debye length, $r_D = 3\sqrt{\mu}$ Å, remembering that these are scaled by the Coulomb distance, $r_C = 540/\epsilon$ Å. If this ratio is large, the discrete charge model is preferable and vice versa for small values of this ratio: it is a question of overlapping Coulomb fields versus screening by mobile charge.

Interfacial Barriers

One cannot yet cleanly separate out the various factors affecting the second-order rate constant in the interfacial region, such as electrostatics, chemistry, i.e., orbital structure, distance, and orientation of reactants. However, that simple kinetics are observed up to the 4-ns risetime shows clearly that there are no large interfacial barriers to molecular movement. It has been postulated that there exist layers of tightly bonded water at the lipid bilayer–water interface (Hauser and Phillips, 1979; Luzar et al., 1984; Prats et al., 1986) or that the polar headgroup region is highly ordered and thus rigid. Our experiments clearly show that the structure at the interface is evanescent on the nanosecond time scale. The structure that is undoubtedly present is highly dynamic. Because the electron transfer can occur through a distance of ~5 Å on these time scales (Mauzerall, 1976), lack of motion over this range cannot be excluded. A decrease of the present time limit of these measurements and their extension to proton transfer reactions should allow further exploration of these dynamic processes at the lipid bilayer–water interface. Such a decrease is possible by the availability of faster amplifiers and by iterative convolution of the system response with kinetic models of the photovoltage.

We thank Ms. Irene Zielinski-Large for technical assistance and the U.S. Public Health Service for support through grant GM-25693.

Received for publication 14 April 1987 and in final form 26 June 1987.

REFERENCES

Ballard, S. G., and D. Mauzerall. 1980. Photochemical ionogenesis in solution of zinc octaethyl porphyrins. *J. Chem. Phys.* 72:933–947.

Carapellucci, P. A., and D. Mauzerall. 1975. Photosynthesis and porphyrin excited state redox reaction. *Ann. NY Acad. Sci.* 244:214–238.

Cherry, R. J., K. Hsu, and D. Chapman. 1972. Polarised absorption spectroscopy of chlorophyll-lipid membranes. *Biochim. Biophys. Acta.* 267:512–522.

Dannhauser, T. J., M. Nango, N. Oku, K. Anzai, and P. A. Loach. 1986. Transmembrane electron transfer as catalyzed by poly(ethylenimine)-linked manganese porphyrins. *J. Am. Chem. Soc.* 108:5865–5871.

Davis, J. H. 1983. The description of membrane lipid conformation, order and dynamics by H-NMR. *Biochim. Biophys. Acta.* 737:117–171.

Debye, P. 1942. Reaction rates in ionic solutions. *Trans. Electrochem. Soc.* 82:265–269.

Feitelson, J., and N. Barboy. 1986. Triplet-state reactions of zinc protoporphyrins. *J. Phys. Chem.* 90:271–274.

Fendler, J. H. 1984. Interactions and kinetics in membrane mimetic systems. *Annu. Rev. Phys. Chem.* 35:137–157.

Flewelling, R. F., and W. L. Hubbell. 1986. The membrane dipole potential in a total membrane potential model. *Biophys. J.* 49:541–552.

Ford, W. E., and G. Tollin. 1986*a*. Chlorophyll photosensitized electron transfer in phospholipid bilayer vesicle systems: correlations between kinetic parameters and solubilities of viologen acceptors. *Photochem. Photobiol.* 43:319–330.

Ford, W. E., and G. Tollin. 1986*b*. Chlorophyll photosensitized electron transfer in phospholipid bilayer vesicle systems: secondary oxidation or reduced viologen acceptors by $Ru(NH_3)_6^{3+}$. *Photochem. Photobiol.* 43:467–473.

Harriman, A., G. Porter, and P. Walters. 1983*a*. Photo-oxidation of metalloporphyrins in aqueous solution. *J. Chem. Soc. Faraday Trans.* 79:1335–1350.

Harriman, A., G. Porter, and A. Wilowska. 1983*b*. Photoreduction of benzo-1,4-quinone sensitized by metalloporphyrins. *J. Chem. Soc. Faraday Trans.* 79:807–816.

Hauser, H., and M. C. Phillips. 1979. Interactions of the polar groups of phospholipid bilayer membranes. *Prog. Surf. Membr. Sci.* 13:297–413.

Hong, F. T. 1976. Charge transfer across pigmented bilayer lipid membrane and its interfaces. *Photochem. Photobiol.* 24:155–189.

Hong, F. T., and D. Mauzerall. 1972. Photo emf at a single membrane-solution interface specific to lipid bilayers containing magnesium porphyrins. *Nature New Biol.* 240:154–155.

Hong, F. T., and D. Mauzerall. 1974. Interfacial photoreactions and chemical capacitance in lipid bilayer. *Proc. Natl. Acad. Sci. USA.* 71:1564–1568.

Hong, F. T., and D. Mauzerall. 1976. Tunable voltage clamp method: application to photoelectric effects in pigmented bilayer lipid membranes. *J. Electrochem. Soc.* 123:1317–1324.

Huang, C., and J. P. Charlton. 1972. Interactions of phosphatidylcholine vesicles with 2-p-toluidinylnaphthalene-6-sulfonate. *Biochemistry.* 11:735–740.

Ilani, A., T. M. Liu, and D. Mauzerall. 1985. The effect of oxygen on the amplitude of photodriven electron transfer across the lipid bilayer-water interface. *Biophys. J.* 47:679–684.

Ilani, A., and D. Mauzerall. 1981. The potential span of photoredox reactions of porphyrins and chlorophyll at the lipid bilayer-water interface. *Biophys. J.* 35:79–92.

Kano, K., and T. Mastuo. 1974. Photochemistry in micellar system. I. Stabilization of the radical anions of antraquinonesufonates. *Bull. Chem. Soc. Japn.* 47:836–842.

Liu, T. M., and D. Mauzerall. 1985. Distributed kinetics of decay of the photovoltage at the lipid bilayer-water interface. *Biophys. J.* 48:1–7.

Luzar, A., S. Svetina, and B. Zebs. 1984. Polarization of water at the solid liquid interface. *Bioelectrochem. Bioeng.* 13:473–484.

Mauzerall, D. 1976. Electron-transfer reactions and photoexcited porphyrins. Chlorophyll-proteins reaction centers and photosynthetic membranes. *Brookhaven Symp. Biol.* 28:64–73.

Mauzerall, D., and S. G. Ballard. 1982. Ionization in solution by photoactivated electron transfer. *Annu. Rev. Phys. Chem.* 33:377–407.

McLaughlin, S. 1977. Electrostatic potentials at membrane-solution interfaces. *Curr. Top. Membr. Transp.* 71–144.

Mueller, P., D. O. Rudin, H. T. Tien, and W. C. Wescott. 1963. Methods for the formation of single bimolecular lipid membranes in aqueous solution. *J. Phys. Chem.* 67:534–535.

Nahor, G. S., and J. Rabani. 1985. Charge separation and photoreduction of zinc tetrakis (sulfonato-phenyl) porphyrin by nitrobenzene and methyl viologen in aqueous solutions. *J. Phys. Chem.* 89:2468–2472.

Prats, M., J. Teissie, and J.-J. Tocanne. 1986. Lateral proton conduction at lipid-water interfaces and its implications for the chemiosmotic-coupling hypothesis. *Nature (Lond.).* 322:756–758.

Raudino, A., and D. Mauzerall. 1986. Dielectric properties of the polarhead group region of zwitterionic lipid bilayers. *Biophys. J.* 50:441–449.

Senthilathipan, V., and G. Tollin. 1985. Light-induced electron transfer reactions between chlorophyll and electrically charged acceptors in positively and negatively charged lipid bilayer vesicles. *Photochem. Photobiol.* 42:437–446.

Smith, R. L., and E. Oldfield. 1984. Dynamic structure of membranes by Deuterium NMR. *Science (Wash. DC).* 225:280–288.

Tien, H. T., and N. B. Joshi. 1986. Photoinitiated electron transfer processes on and across bilayer lipid membranes. *Photobiochem. Photobiophys.* 10:241–251.

Varnardore, W. E., Jr., R. T. Arrieta, J.-R. Duchek, and J. S. Huebner. 1982. Erythrosin and pH gradient induced photo-voltages in bilayer membranes. *J. Membr. Biol.* 65:147–153.

Watts, A., and T. W. Poile. 1986. Direct determination by ^{2}H-NMR of the ionization state of phospholipids and of a local anaesthetic at the membrane surface. *Biochim. Biophys. Acta.* 861:368–392.

Woodle, M., and D. Mauzerall. 1986. Photoinitiated ion movements in bilayer membranes containing magnesium octaethyl-porphyrin. *Biophys. J.* 50:431–439.